Am J Physiol Lung Cell Mol Physiol 297: L1170–L1178, 2009.
First published October 9, 2009; doi:10.1152/ajplung.00168.2009.

Age-dependent endothelial nitric oxide synthase uncoupling in pulmonary arteries of endoglin heterozygous mice

J. Belik,[1,4,6] M. Jerkic,[2,4,6] B. A. S. McIntyre,[1,4] J. Pan,[1,4] J. Leen,[2] L. X. Yu,[3,5] R. M. Henkelman,[3,5] M. Toporsian,[7] and M. Letarte[2,4,6]

[1]*Physiology and Experimental Medicine and* [2]*Molecular Structure and Function Program,* [3]*Mouse Imaging Centre, The Hospital for Sick Children,* [4]*Department of Pediatrics and* [5]*Medical Biophysics,* [6]*Heart and Stroke Richard Lewar Center of Excellence, University of Toronto, Toronto, Ontario, Canada; and* [7]*Beth Israel Deaconess Medical Center, Boston, Massachusetts*

Submitted 22 May 2009; accepted in final form 6 October 2009

Belik J, Jerkic M, McIntyre BA, Pan J, Leen J, Yu LX, Henkelman RM, Toporsian M, Letarte M. Age-dependent endothelial nitric oxide synthase uncoupling in pulmonary arteries of endoglin heterozygous mice. *Am J Physiol Lung Cell Mol Physiol* 297: L1170–L1178, 2009. First published October 9, 2009; doi:10.1152/ajplung.00168.2009.—Endoglin is a TGF-β superfamily receptor critical for endothelial cell function. Mutations in this gene are associated with hereditary hemorrhagic telangiectasia type I (HHT1), and clinical signs of disease are generally more evident later in life. We previously showed that systemic vessels of adult *Eng* heterozygous ($Eng^{+/-}$) mice exhibit increased vasorelaxation due to uncoupling of endothelial nitric oxide synthase (eNOS). We postulated that these changes may develop with age and evaluated pulmonary arteries from newborn and adult $Eng^{+/-}$ mice for eNOS-dependent, acetylcholine (ACh-induced) vasorelaxation, compared with that of age-matched littermate controls. While ACh-induced vasorelaxation was similar in all newborn mice, it was significantly increased in the adult $Eng^{+/-}$ vs. control vessels. The vasodilatory responses were inhibited by L-NAME suggesting eNOS dependence. eNOS uncoupling was observed in lung tissues of adult, but not newborn, heterozygous mice and was associated with increased production of reactive O_2 species (ROS) in adult $Eng^{+/-}$ vs. control lungs. Interestingly, ROS generation was higher in adult than newborn mice and so were the levels of NADPH oxidase 4 and SOD 1, 2, 3 isoforms. However, enzyme protein levels and NADPH activity were normal in adult $Eng^{+/-}$ lungs indicating that the developmental maturation of ROS generation and scavenging cannot account for the increased vasodilatation observed in adult $Eng^{+/-}$ mice. Our data suggest that eNOS-dependent H_2O_2 generation in $Eng^{+/-}$ lungs accounts for the heightened pulmonary vasorelaxation. To the extent that these mice mimic human HHT1, age-associated pulmonary vascular eNOS uncoupling may explain the late childhood and adult onset of clinical lung manifestations.

lung; newborn; pulmonary vascular resistance; hereditary hemorrhagic telangiectasia

LUNG BLOOD FLOW IS MOSTLY dependent on the regional arteriolar and venular intraluminal diameter that ultimately determines the pulmonary vascular resistance (PVR). Nitric oxide (NO) is constitutively produced by endothelial and smooth muscle cells (39) via synthases (NOS) of which there are three isoforms: endothelial (eNOS), neuronal (nNOS), and inducible (iNOS). Although there is evidence that iNOS and nNOS are expressed in the fetal pulmonary vasculature (38), lung eNOS protein expression increases during gestation suggesting that its vascular tissue content and/or activity is in part responsible for the high PVR prenatally and the changes occurring after birth (15). In sheep, lung eNOS expression is maximal in late gestation (34), whereas in rats it is highest either before (33), or immediately after, birth (23). Postnatally, lung vascular tissue eNOS expression was shown to decrease with age in pigs (17).

eNOS converts L-arginine to L-citrulline to generate NO. Its activity is dependent on Ca^{2+}/calmodulin (CaM), but also on subcellular localization, posttranslational modifications, and interaction with several regulatory proteins, including Hsp90 (11, 14). Hsp90 facilitates CaM-induced release from caveolae and acts as a scaffold factor for eNOS; it is necessary for eNOS phosphorylation at Ser1177 (13, 43). This complex process controls the state of eNOS activation and the fidelity of NADPH-dependent electron flux from the reductase to the oxygenase domain, where NO synthesis occurs. Reduced availability of the substrate L-arginine (47), or the cofactor tetrahydrobiopterin (BH_4) (46), as well as changes in Hsp90-eNOS interactions (36) or Thr495 dephosphorylation (27), can uncouple the electron transfer reactions and result in the production of superoxide instead of NO. eNOS is then said to be uncoupled. Under these conditions, superoxide is quickly converted into peroxynitrite if NO is also present locally, or into H_2O_2 via superoxide dismutase (SOD) (22). H_2O_2 is converted into H_2O and O_2 by catalase and glutathione peroxidase (9).

Our recent studies (44) reported that endoglin, a coreceptor of the TGF-β superfamily primarily expressed in endothelial cells, associates with eNOS and Hsp90 and stabilizes the activation complex, resulting in NO production (44). *Endoglin (Eng)* null mice die at midgestation of cardiovascular defects, whereas heterozygous ($Eng^{+/-}$) mice are models of hereditary hemorrhagic telangiectasia (HHT) type 1 (2, 41). We have previously shown that eNOS activity is uncoupled in systemic resistance arteries of $Eng^{+/-}$ mice (44).

Lung vascular abnormalities are observed in HHT patients. Pulmonary arteriovenous malformations are much more frequent in HHT1 than in the general population and in HHT1 vs. HHT2 patients (5, 25). Subjects with HHT most commonly manifest pulmonary symptoms and other signs of disease including epistaxis and telangiectases later in childhood and adult life (5, 45), suggesting that the clinical consequences of *ENG* mutations are more readily manifested with aging.

The purpose of the present study was to compare newborn and adult $Eng^{+/-}$ pulmonary arteries to those of age-matched littermate controls in terms of vasorelaxation, eNOS uncoupling, superoxide production, and levels of enzymes responsible for synthesis and degradation of superoxide. Confirming

Address for reprint requests and other correspondence: J. Belik, The Hospital for Sick Children, 555 Univ. Ave., Toronto, Ontario, M5G 1X8 Canada (e-mail: Jaques.Belik@SickKids.ca).

our hypothesis, the data from this study show that eNOS uncoupling, and not the age-related changes in superoxide generation/degradation, can account for the heightened pulmonary vasorelaxation observed in adult, but not newborn, *Eng* heterozygous mice.

METHODS

Mice. N17-N19 $Eng^{+/-}$ and $Eng^{+/+}$ mice were generated by successive backcrosses onto the C57BL/6 background. All procedures were conducted according to criteria established by the Canadian Council on Animal Care and were approved by The Hospital for Sick Children Research Institute Animal Care Committee. The pups were reared with their mothers and studied between 5–8 days of age (earliest age that allows for successful dissection of near-resistance pulmonary arteries), whereas adults were tested at 8–12 wk. Mice were killed by pentobarbital sodium overdose, and the lungs were extracted immediately after death, rapidly and passively drained of blood, and maintained on cold Krebs-Henseleit solution for biochemical assays and dissection of pulmonary arteries. Lungs were also perfused and snap-frozen for subsequent measurements of reactive oxygen species (ROS) generation and enzyme protein levels.

Organ bath studies. Third-generation lung intralobar pulmonary artery ring segments (average diameter 80–100 μm and length = 2 mm) were dissected free from surrounding tissue and mounted in a wire myograph (Danish Myo Technology). Isometric changes were digitized and recorded online (Myodaq, Danish Myo Technology and Aarhus, Denmark). Tissues were bathed in Krebs-Henseleit buffer (115 mM NaCl, 25 mM $NaHCO_3$, 1.38 mM $NaHPO_4$, 2.51 mM KCl, 2.46 mM $MgSO_4$-7 H_2O, 1.91 mM $CaCl_2$, 5.56 mM dextrose), bubbled with air/6% CO_2, and maintained at 37°C. After a 1-h equilibration, the optimal tissue resting tension was determined by repeated stimulation with 128 mM KCl until maximum active tension was reached. All subsequent force measurements were obtained at optimal resting tension.

Pulmonary vascular muscle force generation was evaluated by stimulating with either the thromboxane A_2-mimetic U46619 or phenylephrine (adult vessels). Contractile responses were normalized to the tissue cross-sectional area as follows: (width × diameter) × 2 and expressed as mN/mm^2. Relaxation was induced with the endothelium-dependent and -independent agonists ACh and sodium nitroprusside (SNP), respectively, following precontraction with U46619 or phenylephrine (adult) at concentrations equivalent to 75% of the maximal agonist-induced contraction (EC_{75}). The nonspecific NOS inhibitor L-NAME was used at 10^{-4} M concentration.

Vessel measurements by X-ray micro-computerized tomography and morphometry. Anaesthetized mice were intubated by tracheotomy, and breathing was supported using a pressure-controlled ventilator. Mice were perfused at 20 mmHg via the right ventricle with warm heparinized PBS followed by Microfil (Flow Tech) at 40 mmHg, using a pressure Servo System PS/200 (Living Systems Instrumentation). Specimens were scanned at 29 μm using a Micro-CT scanner (GE Healthcare). Three-dimensional volume data were reconstructed using the Feldkamp algorithm for cone beam CT geometry. The pulmonary arterial internal diameters of the first three generation vessels (main pulmonary artery considered as first generation) were measured using Display and Amira software (TGS, Berlin, Germany) in three mice of each genotype. Images were rotated to clearly determine wall boundaries of the vessels.

Paraffin-embedded transverse lung sections of five 8- to 12-wk-old mice of each genotype were stained with Movat pentachrome, and five independent fields were quantified using Openlab software (Florence, Italy). Morphometric analysis of pulmonary arterial vessels (60–120 μm) was obtained at ×100 magnitude, and the inner diameter of 20 randomly selected vessels (from 6–7 fields) was measured.

Preparation of tissue extracts. Lung extracts were prepared in lysis buffer consisting of 50 mM Tris·HCl, pH 7.5, 150 mM NaCl, 1.5 mM $MgCl_2$, 0.1% SDS, 0.5% deoxycholate, 1% Nonidet P-40 (or Triton X-100), 1 mM PMSF, and complete protease inhibitors (Roche). Lung tissue was homogenized in a rotor/stator type homogenizer while pulmonary arteries and bronchi were frozen in liquid nitrogen and ground with mortar and pestle before ice-cold lysis buffer was added.

After 1 h on ice, the homogenates were centrifuged at 13,000 *g* for 20 min, and the supernatants were collected. Total protein concentration was measured according to the Bradford method (3); extracts were diluted to a final protein concentration of 4 mg/ml.

Immunoblotting studies. Tissue extracts were incubated in Laemmli buffer at 100°C for 5 min and electrophoresed on 4–12% gradient SDS/PAGE gels. Fractionated proteins were electrotransferred to nitrocellulose membranes (Amersham Biosciences, Mississauga, Canada) at 4°C for 1 h at a constant voltage of 100 V. Membranes were blocked with 2% fish gelatin or 5% milk in TBS-T (20 mM Tris, pH 7.6, 137 mM NaCl, 0.1% Tween 20) for 1 h at 23°C. The blots were incubated at 4°C overnight with commercially available antibodies as follows: CD105/endoglin, rat IgG2a clone MJ7/18, 1:500 dilution (Southern Biotech, Birmingham, AL); eNOS 1:3,000, Hsp90 1:1,000, and

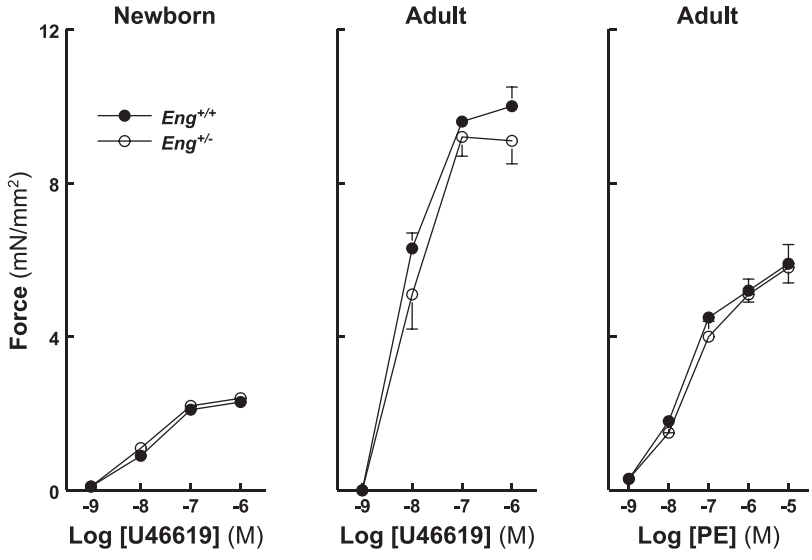

Fig. 1. Force generation in response to agonist stimulation. Thromboxane A_2 analog U46619 or phenylephrine (PE; adult)-induced force generation of pulmonary arteries obtained from adult $Eng^{+/+}$ (n = 15–16), $Eng^{+/-}$ (n = 16–19), newborn $Eng^{+/+}$ (n = 15), $Eng^{+/-}$ (n = 12). No genotype-dependent difference in agonist-induced force dose-response curves was noted for the newborn and adult arteries.

gp91phox/Nox2 1:1,000 (mouse IgG1; BD Biosciences, Mississauga, ON); SOD1 1:4,000, catalase 1:2,000, and SOD3/EC-SOD 1:3,000 (goat IgG, R&D, Minneapolis, MN); Nox4, rabbit IgG, 1:200 (Lab Vision, Fremont, CA); SOD2, rabbit IgG, 1:3,000 (Lifespan Biosciences, Seattle, WA).

After being washed with TBS-T for 30 min, the blots were incubated with IgG conjugated with horseradish peroxidase (1:20,000 dilution in TBS-T containing 5% milk) for 60 min and washed again with TBS-T for 40 min, all at 23°C. The enhanced chemiluminescence (ECL; Perkin Elmer, Shelton, CT) reagent was used for detection. The membrane blots were stripped and tested with antibodies to β-actin (Sigma Aldrich; dilution 1:40,000).

eNOS-Hsp90 association and immunoblotting. Lungs were excised, cut into 5-mm segments, equilibrated for 2 h in serum-free MCDB 131 media, and stimulated with vehicle or 1 μM ionomycin for 15 min. Samples were washed in PBS, and extracts were prepared in 10 mmol/l Tris·HCl, pH 7.4 (1% Triton X-100 with protease and phosphatase inhibitors, Roche Biochemicals). Samples were precleared with protein A/G mixture, and equal protein amounts were immunoprecipitated with anti-eNOS and immunoblotted using Hsp90 and eNOS antibodies. Bands were visualized by chemiluminescence and quantified by densitometry.

H2DCFDA fluorescence and H_2O_2 measurement. Lungs were homogenized in Krebs-Henseleit buffer, pH 7.4, supplemented with 0.1 M $NaHPO_4$ and 1 mM NaN_3, with a buffer to wet tissue weight ratio of 6:1. Homogenates were centrifuged at 13,000 *g* for 15 min. ROS levels in the supernatant were assessed using 10 μmol/l H2DCFDA (Molecular Probes, Invitrogen, Burlington, ON) at 37°C. Fluorescence was quantified on a SpectraMax Gemini EM microplate spectrofluorometer (Molecular Devices, MDS Analytical Technologies, Sunnyvale, CA) using 488-nm excitation and 525-nm emission wavelengths. Levels were normalized per microgram of protein.

$Eng^{+/+}$ and $Eng^{-/-}$ embryonic endothelial cells (35) were grown in Optilux 96-well black clear-bottom plates and serum-starved for 3 h. Cells were incubated with 5 μmol/l DHE in the presence and absence of ionomycin (5×10^{-7} M), L-NAME (10^{-3} M), or apocyanin (10^{-4} M). Live cells were observed through the CY3 fluorescence channel and photographed using a Nikon TE2000 inverted microscope equipped with an environmental chamber set to 37°C and 5% CO_2. The number of positive nuclei/field was quantified based on size and intensity using Volocity 3D imaging software (Improvision).

H_2O_2 levels in the lung homogenate supernatants were measured using a calibrated H_2O_2 specific sensor (World Precision Instruments, Sarasota, FL). Protein concentrations were measured using the Bradford assay, and H_2O_2 readings were expressed as μmol H_2O_2/g of extract protein.

NADPH oxidase activity. NADPH oxidase activity was measured in the adult mice utilizing the commercially available Cytochrome *C* Reductase (NADPH) Assay Kit (Sigma Aldrich, Oakville, ON) as previously reported by others (16, 32).

Chemicals. Unless otherwise indicated, all chemicals were obtained from Sigma Aldrich.

Data analysis. Data were evaluated by one- or two-way ANOVA with multiple comparisons obtained by the Tukey-Kramer test, when appropriate. Statistical significance was accepted at $P < 0.05$. All statistical analyses were performed with the Number Cruncher Statistical System (Kaysville, UT). Data are presented as means ± SE.

RESULTS

Age differences in pulmonary arterial responses. Force generation, in response to agonist stimulation, was evaluated in newborn and adult pulmonary arteries (Fig. 1). Direct comparison of newborn and adult vessels using the U46619 agonist revealed higher force generation in adults. When comparing the adult $Eng^{+/-}$ arteries vs. those of littermate controls, the phenylephrine (PE) agonist dose-response curves were identical to those observed with U46619. No significant differences in force generated in response to these agonists were observed for the newborn or adult $Eng^{+/-}$ arteries vs. those of littermate controls.

Significant age-related differences were observed in the endothelium-dependent relaxation response of pulmonary arteries from $Eng^{+/-}$ mice compared with control littermates. Whereas the relaxation response was similar in the newborns, ACh induced a significantly greater relaxation in the $Eng^{+/-}$ adult arteries when compared with age-matched control vessels (Fig. 2).

To address the role of eNOS in the heightened vasorelaxation of the adult $Eng^{+/-}$ mice, we measured the pulmonary arterial ACh-induced relaxation response in the presence of L-NAME (10^{-4} M), a NOS inhibitor. L-NAME inhibited the vasorelaxation in all groups of mice, suggesting that the enhanced ACh-induced relaxation in adult heterozygous mice is eNOS dependent (Fig. 2). No significant differences were observed for the endothelium-independent (SNP) relaxation

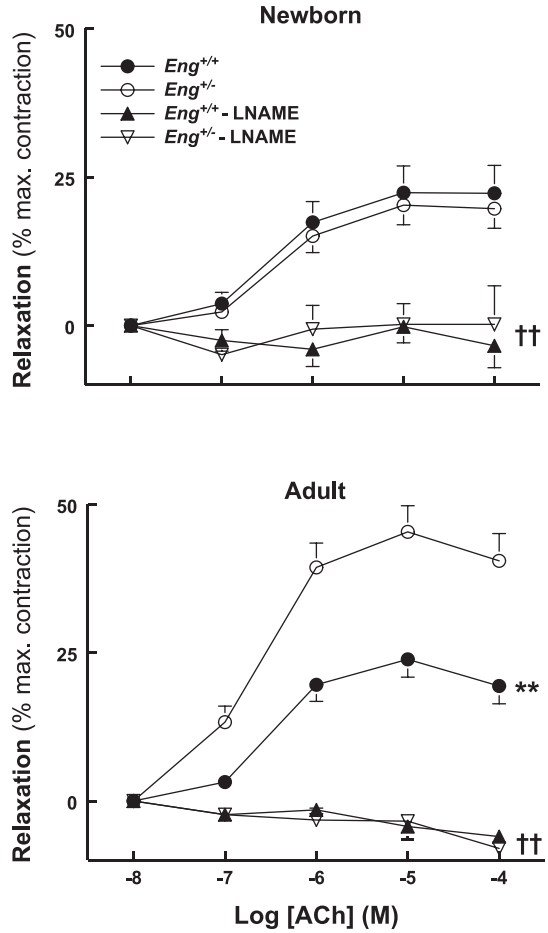

Fig. 2. Age-related differences in endothelium-dependent relaxation. Endothelium-dependent (ACh-induced) relaxation response of U46619 (newborn) or phenylephrine (adult) precontracted (EC_{75}) pulmonary arteries. Control: adult $Eng^{+/+}$ ($n = 55$), $Eng^{+/-}$ ($n = 47$); newborn $Eng^{+/+}$ ($n = 18$), $Eng^{+/-}$ ($n = 17$); L-NAME: adult $Eng^{+/+}$ ($n = 8$), $Eng^{+/-}$ ($n = 8$). $^{**}P < 0.01$ vs. $Eng^{+/+}$; $^{††}P < 0.01$ vs. non L-NAME-treated vessels by 2-way ANOVA and Tukey-Kramer multiple comparison test. Adult, but not newborn, $Eng^{+/-}$ arteries showed increased ACh-induced relaxation compared with $Eng^{+/+}$ arteries.

dose-response curves between $Eng^{+/-}$ pulmonary arteries and controls (Fig. 3). Of note, the SNP, but not the ACh-induced relaxation response, was higher in adult than newborn mice (Figs. 2 and 3). The adult ACh and SNP response patterns between $Eng^{+/-}$ pulmonary arteries and controls were similar when U46619 agonist was used instead of PE (data not shown).

To determine the mechanism accounting for the enhanced vasorelaxation observed in adult $Eng^{+/-}$ mice, we evaluated wild-type newborn and adult mouse pulmonary arterial response to H_2O_2. A similar vasorelaxation dose-response to H_2O_2 was evident for both age groups (Fig. 4).

Increased diameter of large pulmonary arteries in adult $Eng^{+/-}$ mice. To evaluate whether the enhanced vasorelaxation observed in $Eng^{+/-}$ mice resulted in altered vessel diameter, lungs of adult $Eng^{+/-}$ and control mice were imaged by micro CT, and the internal diameter of the pulmonary arteries was measured. A significantly greater ($P < 0.01$) diameter was documented in the $Eng^{+/-}$ first three generation vessels compared with control vessels (Fig. 5). Furthermore, fourth-generation vessels, such as those used for arterial response, were measured on histological sections of perfused lungs. The average inner diameter of the adult $Eng^{+/-}$ mice pulmonary arteries (87.1 ± 0.9 μm; $n = 5$) was significantly greater ($P < 0.001$) than that of control mice (79.5 ± 1.0 μm; $n = 5$).

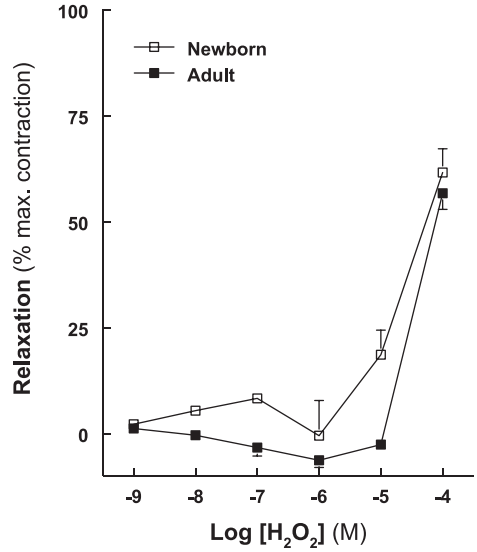

Fig. 4. Vasorelaxation dose response to H_2O_2. H_2O_2 dose-response relaxation of newborn ($n = 4$) and adult ($n = 4$) wild-type C57BL/6 mouse pulmonary arteries precontracted (EC_{75}) with U46619 or phenylephrine, respectively. H_2O_2 is a pulmonary vasorelaxant in newborn and adult mice.

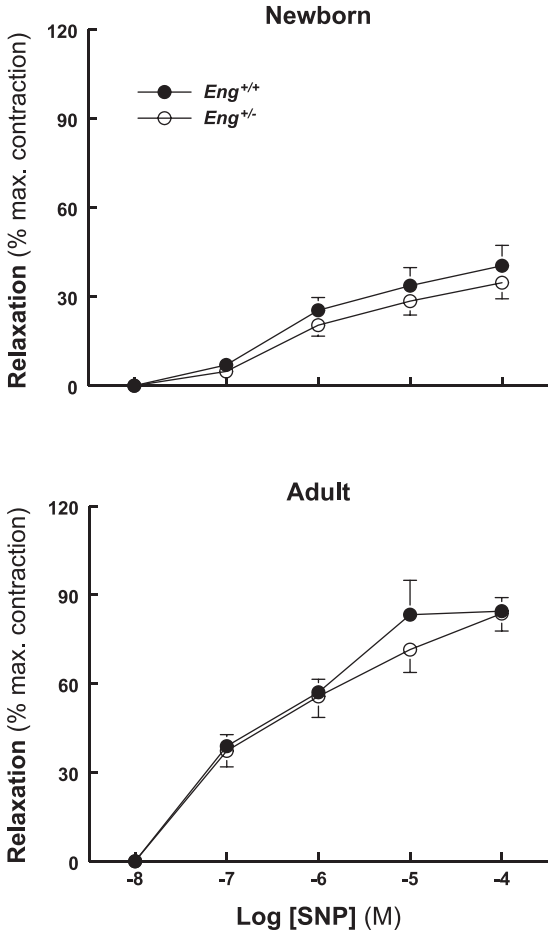

Fig. 3. Age-related differences in endothelium-independent relaxation. Endothelium-independent (SNP-induced) relaxation response of U46619 precontracted (EC_{75}) pulmonary arteries obtained from adult $Eng^{+/+}$ ($n = 10$), $Eng^{+/-}$ ($n = 12$), and newborn $Eng^{+/+}$ ($n = 10$), $Eng^{+/-}$ ($n = 10$). A significant difference was observed in SNP-induced pulmonary arterial vasorelaxation with age but not with genotype.

Hsp90:eNOS association and H_2O_2 generation. As expected for heterozygous mice, the lung tissue content of endoglin was 50% relative to the littermate control group. However, endoglin levels were significantly higher ($P < 0.01$) in the adult vs. newborn mice in both $Eng^{+/-}$ and control groups (Fig. 6). Lung eNOS expression on the contrary decreased with age and was significantly higher in the newborn when compared with adults ($P < 0.05$). No significant genotype-dependent difference in lung eNOS expression was observed at either age in these mice. The expression of lung Hsp90 was unchanged with age in both heterozygous and control mice.

The extent of Hsp90:eNOS association estimated for unstimulated and ionomycin-stimulated lung tissue was similar in $Eng^{+/-}$ and control newborn mice (Fig. 7). In adult lungs, a significant increase in ionomycin-stimulated Hsp90:eNOS association was observed in $Eng^{+/+}$, but not $Eng^{+/-}$, mice. When compared with the adult $Eng^{+/+}$, a lower level of Hsp90:eNOS association was observed for the $Eng^{+/-}$ lungs under basal and stimulated conditions (Fig. 7).

The ROS content, as measured by the H2DCFDA fluorescence assay, was similar in newborn $Eng^{+/-}$ and control lung tissue (Fig. 8*A*). In contrast, the H2DCFDA fluorescence was significantly increased in adult $Eng^{+/-}$ mouse lungs compared with the control group. A significant increase in H2DCFDA fluorescence was also documented in the adult lung tissue when compared with the newborn regardless of genotype (Fig. 8*A*).

We also evaluated the H_2O_2 content in the adult mouse lungs. It was significantly higher in the adult $Eng^{+/-}$ than in the control group (Fig. 8*B*; $P < 0.05$). No differences in lung H_2O_2 levels were observed between $Eng^{+/+}$ and $Eng^{+/-}$ newborn mice.

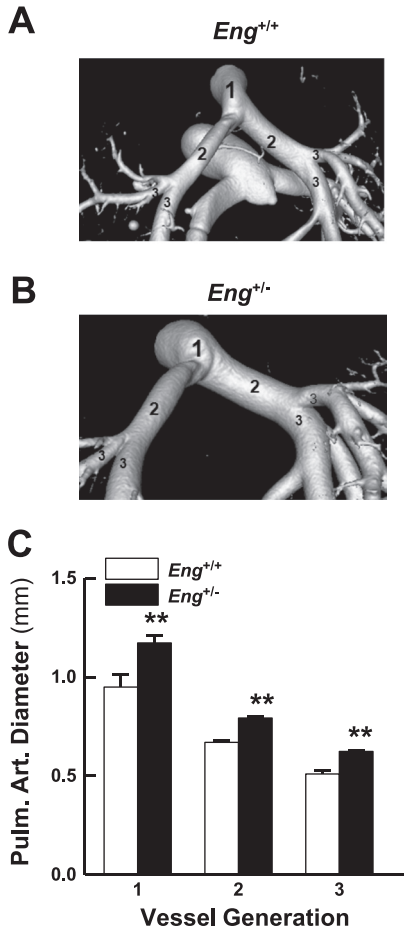

Fig. 5. Measurements of large pulmonary artery diameter by micro-computerized image (Micro-CT) in adult $Eng^{+/+}$ and $Eng^{+/-}$ mice. *A* and *B*: representative Micro-CT image of large pulmonary arterial vessels (1st to 3rd generation) showing increased diameter in $Eng^{+/-}$ mice compared with $Eng^{+/+}$ littermates (*C*). $N = 3$ for each genotype $^{**}P < 0.01$ compared with $Eng^{+/+}$ mouse values by 2-way ANOVA. Large pulmonary arterial vessels have a greater internal diameter in $Eng^{+/-}$ mice than $Eng^{+/+}$ littermates.

NADPH oxidase and SOD lung tissue content. NADPH oxidase activity was measured to address a possible role of this enzyme in the enhanced lung H_2O_2 content in the adult $Eng^{+/-}$ compared with the control group. The lung NADPH oxidase activity was similar for both groups of adult mice (Fig. 8*C*).

No significant differences in the levels of the two NADPH oxidase isoforms most expressed in the lungs (Nox2 and Nox4) were observed when comparing $Eng^{+/-}$ and control mice (Fig. 9). Similarly, the levels of enzymes responsible for superoxide dismutation (SOD isoforms 1, 2, and 3) were not distinct between $Eng^{+/-}$ and control lung samples (Fig. 9).

When the lung content of these enzymes was evaluated across ages, the adult mouse lungs showed a significantly higher ($P < 0.01$) content of Nox4, and all SOD isotypes, compared with the newborn lungs (Fig. 9).

Constitutive eNOS-derived ROS production in Eng-deficient endothelial cells. To evaluate the source and contribution of the eNOS- and Nox-mediated enzymes to ROS production, we utilized embryonic $Eng^{+/+}$ and $Eng^{-/-}$ endothelial cells (35). Compared with mouse $Eng^{+/+}$ endothelial cells, a significantly greater number of $Eng^{-/-}$ cells showed nuclear DHE staining ($P < 0.01$), indicating higher ROS production under basal conditions (Fig. 10). Ionomycin (10^{-6} M) stimulation significantly increased ($P < 0.01$) DHE staining in the $Eng^{+/+}$, but not $Eng^{-/-}$, endothelial cells. To determine the role of eNOS and Nox on ROS production, we tested the effect of inhibitors of both enzymes. In the presence of L-NAME, the constitutive ROS production by $Eng^{-/-}$ cells was significantly reduced ($P < 0.01$), suggesting eNOS dependence. In contrast, Nox inhibition with apocynin did not reduce the $Eng^{-/-}$ nuclear DHE staining, suggesting that Nox is not implicated in this constitutive ROS production (Fig. 10). The SOD mimetic Tempol (10^{-3} M) significantly reduced the basal $Eng^{-/-}$ nuclear DHE staining, further suggesting that superoxide is the main ROS generated by the *Eng*-deficient cells.

DISCUSSION

We documented a significant increase in pulmonary arterial vasorelaxation in adult, but not newborn, *Eng* heterozygous mice. Whereas the pulmonary arteries of newborn $Eng^{+/-}$ mice showed similar vasomotor properties, an enhanced vasorelaxation potential was observed in vessels from $Eng^{+/-}$ adult arteries compared with age-matched control littermates. This increased endothelium-dependent pulmonary arterial re-

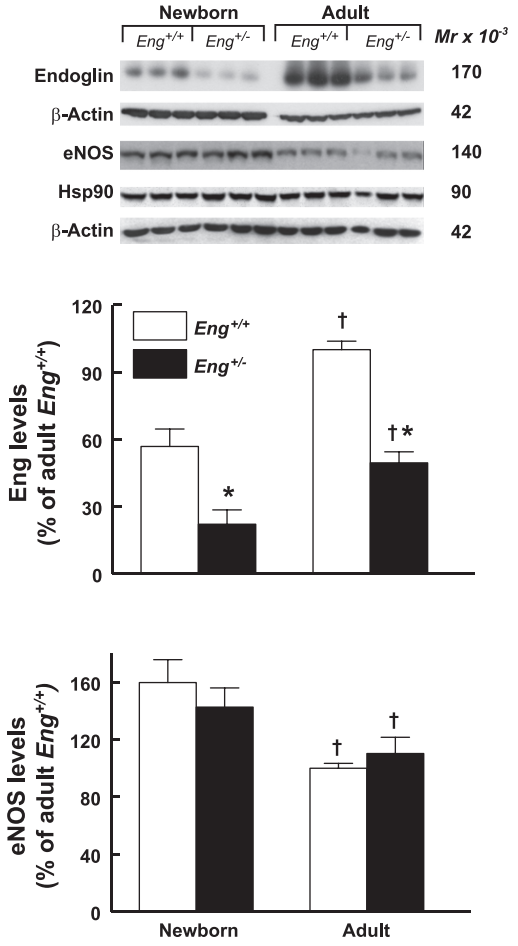

Fig. 6. Levels of endoglin, eNOS, and Hsp90 in lungs of newborn and adult $Eng^{+/+}$ and $Eng^{+/-}$ mice. Representative gels are shown for endoglin (non-reducing conditions), eNOS, Hsp90, and β-actin (reducing conditions) assessed by Western blot. $\dagger P < 0.05$ vs. newborn mice; $^{*}P < 0.05$ vs. $Eng^{+/+}$ adult mice; $n = 20$–30 for eNOS and 12–18 for endoglin.

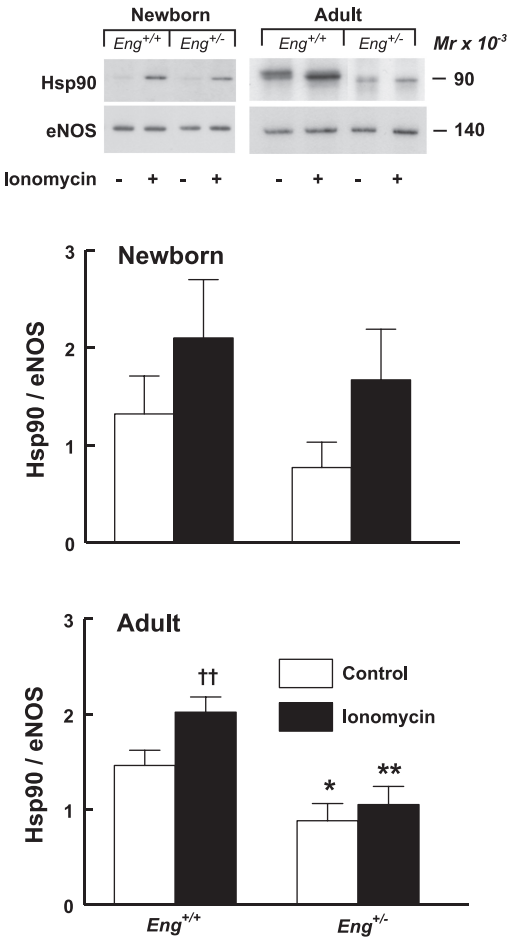

Fig. 7. Coimmunoprecipitation of eNOS with Hsp90 in $Eng^{+/+}$ and $Eng^{+/-}$ adult and newborn mice. Hsp90:eNOS association in lungs of newborn (n = 6) and adult (n = 7) $Eng^{+/+}$ and $Eng^{+/-}$ mice without and with ionomycin (10^{-6} M) stimulation. *$P < 0.05$ and **$P < 0.01$ vs. $Eng^{+/+}$ control and ionomycin-treated, respectively; ††$P < 0.01$ vs. $Eng^{+/-}$ ionomycin stimulated.

laxation was associated with lower basal and stimulated Hsp90:eNOS association levels, as well as increased lung tissue H_2O_2 generation. No significant differences in the levels of expression of the superoxide-producing enzymes Nox2 and Nox4, and of the ROS scavengers SOD and catalase, were documented in the lungs of the $Eng^{+/-}$ mice. Yet, the lung content of Nox4 and SOD1, 2, and 3 isoforms significantly increased with age. Together, these data suggest that the developmentally dependent enhanced eNOS uncoupling, rather than the age-dependent maturation of superoxide-producing and -scavenging enzymes, is the cause of increased endothelium-dependent vasorelaxation in the $Eng^{+/-}$ mice.

Endoglin is a homodimeric glycoprotein (M_r = 180,000) that acts as an ancillary receptor for several TGF-β superfamily ligands. We have previously shown that endoglin associates with eNOS in caveolae and facilitates Hsp90/eNOS association (44). Corroborating this evidence, mesenteric resistance arteries from $Eng^{+/-}$ mice showed enhanced vasodilation that was inhibited by L-NAME and reversed by antioxidant treatment, implying uncoupling of eNOS and eNOS-dependent ROS formation (44).

Little is known about the role of endoglin in the pulmonary vascular tissue and more specifically in the newborn. This protein is present in pulmonary vascular tissue of fetal, premature, and term neonates (1, 10), and its expression increases in infants developing chronic lung disease (7). Given its known angiogenic effects (19), its presence early in life and enhanced expression in normal lungs suggest that endoglin is important for pulmonary vascular development and branching.

As demonstrated for the systemic vessels (44), eNOS uncoupling is the likely cause of increased pulmonary vasorelaxation in the $Eng^{+/-}$ mice. As such, endoglin haploinsufficiency in the adult mice results in increased production of eNOS-dependent superoxide and is then dismutated to higher H_2O_2 content and increased vasorelaxation.

As previously shown by others, H_2O_2 has a vascular dilatory and constricting effect in mice. In the cerebral circulation, H_2O_2 is a vasodilator (8, 9), whereas in renal vessels and aorta,

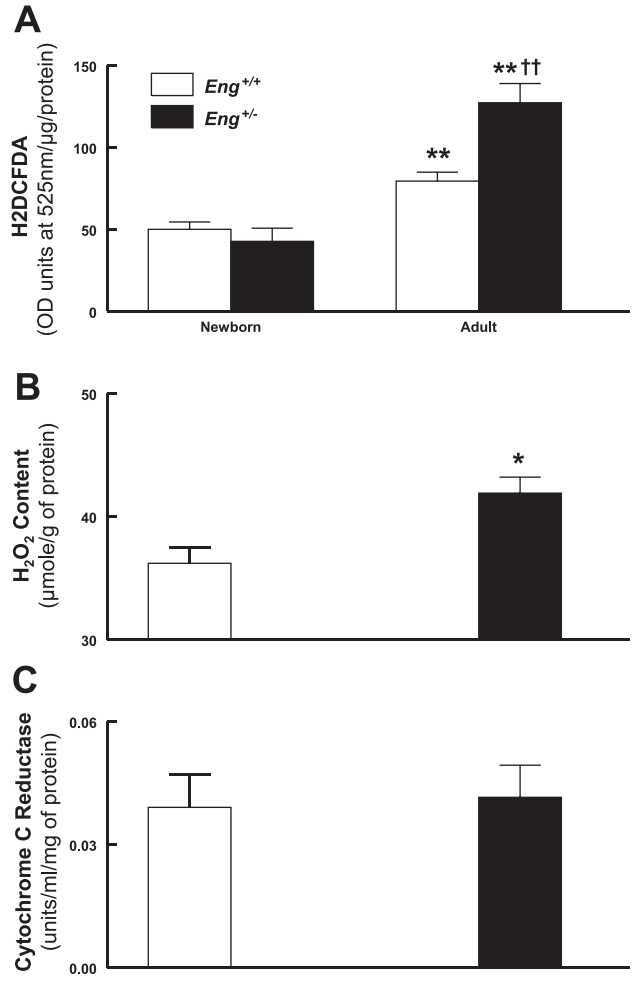

Fig. 8. ROS and NADPH oxidase activity measurements in $Eng^{+/+}$ and $Eng^{+/-}$ adult and newborn mice. *A*: H2DCFDA fluorescence measurements in lung extracts of newborn $Eng^{+/+}$ (n = 15), $Eng^{+/-}$ (n = 4) and adult $Eng^{+/+}$ (n = 18) and $Eng^{+/-}$ (n = 18) mice. **$P < 0.01$ compared with newborn and ††$P < 0.01$ compared with adult $Eng^{+/+}$ mouse lung tissue values. *B*: H_2O_2 content in adult mice (n = 14/group); *$P < 0.05$ compared with $Eng^{+/+}$ values. *C*: lung NADPH oxidase activity measured as cytochrome *c* reduction in adult $Eng^{+/+}$ (n = 4) and $Eng^{+/-}$ (n = 4) mice. When compared with $Eng^{+/+}$, the $Eng^{+/-}$ adult mouse lungs have a higher H_2O_2 content but show no difference in NADPH oxidase activity.

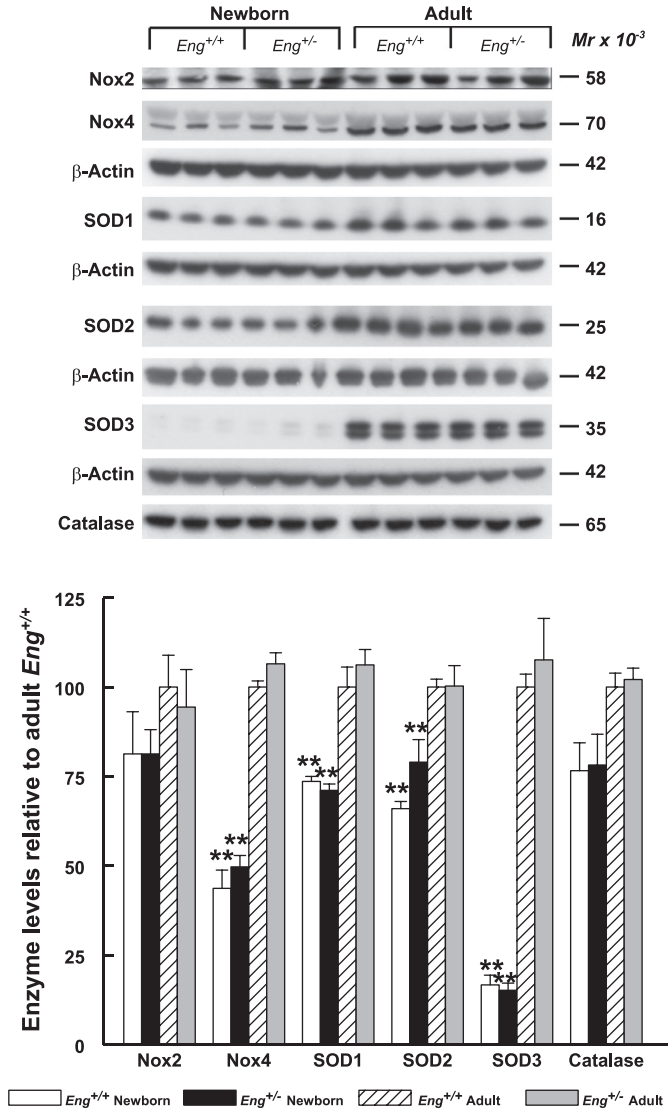

Fig. 9. Nox and SOD protein expression in $Eng^{+/+}$ and $Eng^{+/-}$ adult and newborn mice. Western blot analysis and quantitation of levels of enzymes in lung tissues of $Eng^{+/+}$ and $Eng^{+/-}$ newborn and adult mice as a percentage of adult $Eng^{+/+}$ levels. Representative gels are shown, and average values of all determinations are compiled for the histograms. Nox2 ($n = 6$ per genotype and age group), Nox4 ($n = 9$), SOD1 ($n = 3$), SOD2 ($n = 6$), SOD3 ($n = 6$), and catalase ($n = 3$). $^{**}P < 0.01$ compared with respective adult mouse lung tissue values. Developmental-, but not genotype-, dependent differences in lung enzyme expression were noted.

it exhibits a constrictor effect (12, 42). In the pulmonary circulation, H_2O_2 has been reported to have vasorelaxant and constrictive effects depending on the species and vessel generation (conductance vs. resistance vessels) studied (4, 20, 21, 31, 48).

In the present study, we showed that H_2O_2 has a vasorelaxing effect on the newborn and adult pulmonary arteries. Although this relaxant effect is mostly seen at rather high concentrations, H_2O_2 tissue diffusion in the muscle bath is expected to be low. Whereas small quantities released by the endothelial cells will relax the adjacent smooth muscle in vivo, higher concentrations are likely required under the ex vivo assay conditions to evaluate the H_2O_2 vascular effect.

The lung tissue superoxide content is dependent not only on synthesis but on the expression and activity of enzymes promoting their conversion and degradation, such as SOD and catalase. In the present study, we did not find a significant difference in the expression of these enzymes when comparing lung tissue of $Eng^{+/-}$ and control mice, suggesting that higher levels of H_2O_2 are not due to increased rate of conversion from superoxide in the mutant mice.

It is possible that a more complex process accounts for the increased pulmonary vascular H_2O_2 generation observed in adult $Eng^{+/-}$ mice. In vascular tissue, ACh triggers NO synthesis by eNOS via M_3 subtype muscarinic receptors, but it also induces endothelial H_2O_2 release (26) that was shown to cause relaxation of rat aorta via a calcium- and endothelium-dependent pathway (49). ACh can also trigger H_2O_2 production through NADPH oxidase activation in rat renal arteries (12). ACh induced prostaglandin-independent relaxation in mesenteric arteries of $eNOS^{-/-}$ mice, confirming that it can stimulate H_2O_2 even in the absence of eNOS (29, 30). Yet, in the present study, we demonstrated that eNOS inhibition with L-NAME abolished the ACh-induced relaxation in $Eng^{+/-}$ and control mice, suggesting that the enhanced pulmonary vasodilation of the heterozygous mice is eNOS dependent.

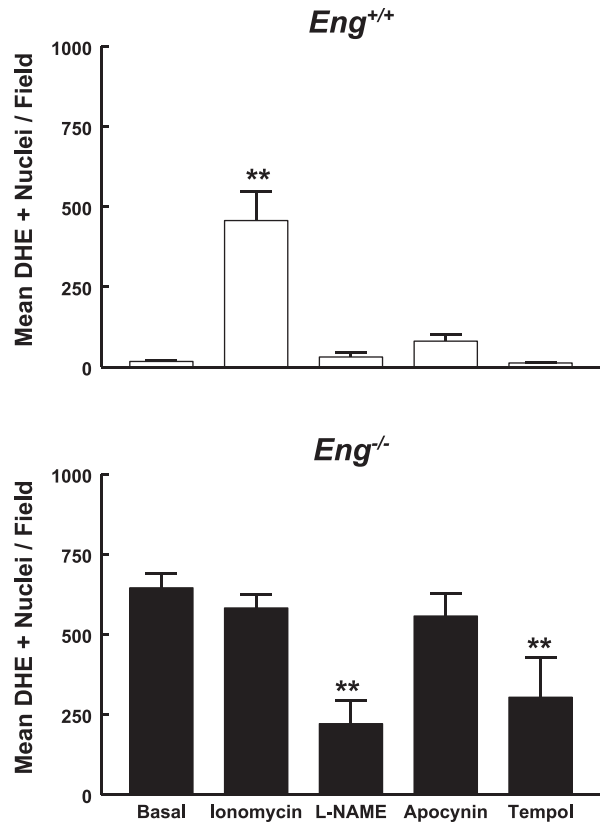

Fig. 10. ROS generation in embryonic $Eng^{+/+}$ and $Eng^{-/-}$ endothelial cells. Endothelial cells were incubated with 5 μmol/l DHE in the presence and absence of ionomycin (5×10^{-7} M), L-NAME (10^{-3} M), apocynin (10^{-4} M), and Tempol (10^{-3} M). Live cells were observed through the CY3 fluorescence channel, and the number of positive nuclei/field was quantified based on size and intensity using Volocity 3D imaging software. $N = 4$ wells for each group. $^{**}P < 0.01$ compared with basal levels by 1-way ANOVA and Tukey-Kramer multiple comparison testing. $Eng^{+/-}$ cells basal mean DHE staining is significantly greater ($P < 0.01$) when compared with $Eng^{+/+}$ cells by unpaired Student's t-test.

The enhanced ACh-induced relaxation observed in lungs of adult $Eng^{+/-}$ mice is not related to NADPH oxidase. Such conclusion is based on the following data. The expression of Nox2 and Nox4, the two most commonly found NADPH oxidase enzyme isoforms in the lung, was similar in $Eng^{+/-}$ and control mice. The lung NADPH oxidase activity was similar in the heterozygous vs. control adult mice. Furthermore, when ROS generation was evaluated in $Eng^{+/+}$ and $Eng^{-/-}$ embryonic endothelial cells, we observed that $Eng^{-/-}$ cells produced much higher levels of constitutive ROS ($P < 0.01$) when compared with $Eng^{+/+}$ cells. Treatment with the NOS inhibitor significantly diminished ROS generation, whereas the Nox inhibitor had no effect, suggesting that superoxide production is eNOS dependent and Nox independent in $Eng^{-/-}$ cells.

Mutations in the *ENG* gene, leading to haploinsufficiency and a nonfunctional protein, are the underlying cause of HHT1 and the predominant predisposing factor for pulmonary arteriovenous malformations. These are most commonly diagnosed in late childhood and adult ages (5, 25, 37). We speculate that endoglin deficiency contributes to pulmonary arteriovenous malformations via increased eNOS-derived ROS and consequent H_2O_2 production, leading to enhanced focal vasorelaxation, as well as vascular tissue damage. In the present study, we documented that $Eng^{+/-}$ adult pulmonary arteries have a larger diameter when compared with those of controls, further supporting the evidence for greater pulmonary vasodilation in *Eng* haploinsufficient mice.

We have previously published that urinary and plasma concentrations of nitrites, a NO metabolite, are lower in $Eng^{+/-}$ than in $Eng^{+/+}$ mice (18). Systemic resistance vessels from $Eng^{+/-}$ mice showed increased ROS generation and abnormal vasomotor function that was corrected following administration of the ROS scavenger Tempol (44). Together, these data are highly suggestive of eNOS uncoupling-induced vascular ROS generation. The antioxidant *N*-acetylcysteine has shown significant beneficial effects in HHT1 subjects with epistaxis suggesting that oxidative stress contributes to the clinical manifestations (6).

In the present study, no significant difference in the endothelium-dependent relaxation potential was observed when comparing newborn $Eng^{+/-}$ and control mice. In keeping with eNOS uncoupling being the causative factor responsible for increased vasorelaxation in adult mice, Hsp90:eNOS association, a marker of enzyme coupling, was significantly decreased in the adult $Eng^{+/-}$ mice compared with age-matched controls. Yet, no difference in Hsp90:eNOS association levels was observed in $Eng^{+/-}$ and control newborns, suggesting that eNOS is coupled early in life, even when endoglin levels are reduced. Such age-dependent difference in the potential for eNOS uncoupling may relate to developmental changes in tetrahydrobiopterin (BH_4) regulation. There is no evidence of Hsp90 involvement in NADPH oxidase-dependent superoxide generation.

Endothelial BH_4 availability is critical for pulmonary vascular NO generation and maintenance of lung vascular homeostasis (24). Developmentally, the serum and urine biopterin levels are highest early in life and decrease with age (40). These age-dependent changes have been shown to play a role in the maintenance of eNOS-coupled state during fetal and newborn life. In sheep, pulmonary arterial eNOS stimulation produces superoxide and H_2O_2 in 4-wk-old, but not fetal, animals, indicating an age-dependent transition from coupling to uncoupling of this enzyme (28). Further investigation of these developmental differences is warranted for the better understanding of the uncoupling process and possible prevention and treatment of the pulmonary pathology in HHT patients.

In summary, we showed that *Eng* haploinsufficiency results in pulmonary vascular eNOS uncoupling in the adult, but not newborn, mice. Pulmonary arteries from adult $Eng^{+/-}$ mice are more dilated and have an enhanced endothelium-dependent smooth muscle relaxation potential. This increased vasorelaxation may play a role in the formation of pulmonary arteriovenous malformations later in life and may explain the generally late onset of pulmonary clinical manifestations in HHT.

GRANTS

This work was supported by Heart and Stroke Foundation of Canada Grants NA 6217 (to J. Belik) and T5598 (to M. Letarte).

DISCLOSURES

No conflicts of interest are declared by the author(s).

REFERENCES

1. **Barresi V, Grosso M, Vitarelli E, Granese R, Barresi G.** Endoglin (CD105) immuno-expression in human foetal and neonatal lungs. *Histol Histopathol* 23: 701–708, 2008.
2. **Bourdeau A, Dumont DJ, Letarte M.** A murine model of hereditary hemorrhagic telangiectasia. *J Clin Invest* 104: 1343–1351, 1999.
3. **Bradford MM.** A rapid and sensitive method for the quantitation of microgram quantities of protein utilizing the principle of protein-dye binding. *Anal Biochem* 72: 248–254, 1976.
4. **Cosentino F, Barker JE, Brand MP, Heales SJ, Werner ER, Tippins JR, West N, Channon KM, Volpe M, Luscher TF.** Reactive oxygen species mediate endothelium-dependent relaxations in tetrahydrobiopterin-deficient mice. *Arterioscler Thromb Vasc Biol* 21: 496–502, 2001.
5. **Cottin V, Dupuis-Girod S, Lesca G, Cordier JF.** Pulmonary vascular manifestations of hereditary hemorrhagic telangiectasia (rendu-osler disease). *Respiration* 74: 361–378, 2007.
6. **de Gussem EM, Snijder RJ, Disch FJ, Zanen P, Westermann CJ, Mager JJ.** The effect of *N*-acetylcysteine on epistaxis and quality of life in patients with HHT: a pilot study. *Rhinology* 47: 85–88, 2009.
7. **De Paepe ME, Patel C, Tsai A, Gundavarapu S, Mao Q.** Endoglin (CD105) up-regulation in pulmonary microvasculature of ventilated preterm infants. *Am J Respir Crit Care Med* 178: 180–187, 2008.
8. **Drouin A, Thorin E.** Flow-induced dilation is mediated by Akt-dependent activation of endothelial nitric oxide synthase-derived hydrogen peroxide in mouse cerebral arteries. *Stroke* 40: 1827–1833, 2009.
9. **Drouin A, Thorin-Trescases N, Hamel E, Falck JR, Thorin E.** Endothelial nitric oxide synthase activation leads to dilatory H_2O_2 production in mouse cerebral arteries. *Cardiovasc Res* 73: 73–81, 2007.
10. **ejandre-Alcazar MA, Michiels-Corsten M, Vicencio AG, Reiss I, Ryu J, de Krijger RR, Haddad GG, Tibboel D, Seeger W, Eickelberg O, Morty RE.** TGF-beta signaling is dynamically regulated during the alveolarization of rodent and human lungs. *Dev Dyn* 237: 259–269, 2008.
11. **Fleming I, Busse R.** Molecular mechanisms involved in the regulation of the endothelial nitric oxide synthase. *Am J Physiol Regul Integr Comp Physiol* 284: R1–R12, 2003.
12. **Gao YJ, Lee RM.** Hydrogen peroxide is an endothelium-dependent contracting factor in rat renal artery. *Br J Pharmacol* 146: 1061–1068, 2005.
13. **Gonzalez E, Kou R, Lin AJ, Golan DE, Michel T.** Subcellular targeting and agonist-induced site-specific phosphorylation of endothelial nitric-oxide synthase. *J Biol Chem* 277: 39554–39560, 2002.
14. **Govers R, Bevers L, de Bree P, Rabelink TJ.** Endothelial nitric oxide synthase activity is linked to its presence at cell-cell contacts. *Biochem J* 361: 193–201, 2002.
15. **Guembe L, Villaro AC.** Histochemical demonstration of neuronal nitric oxide synthase during development of mouse respiratory tract. *Am J Respir Cell Mol Biol* 20: 342–351, 1999.

16. **Han JF, Wang SL, He XY, Liu CY, Hong JY.** Effect of genetic variation on human cytochrome p450 reductase-mediated paraquat cytotoxicity. *Toxicol Sci* 91: 42–48, 2006.
17. **Hislop AA, Springall DR, Buttery LD, Pollock JS, Haworth SG.** Abundance of endothelial nitric oxide synthase in newborn intrapulmonary arteries. *Arch Dis Child Fetal Neonatal Ed* 73: F17–F21, 1995.
18. **Jerkic M, Rivas-Elena JV, Prieto M, Carron R, Sanz-Rodriguez F, Perez-Barriocanal F, Rodriguez-Barbero A, Bernabeu C, Lopez-Novoa JM.** Endoglin regulates nitric oxide-dependent vasodilatation. *FASEB J* 18: 609–611, 2004.
19. **Jerkic M, Rodriguez-Barbero A, Prieto M, Toporsian M, Pericacho M, Rivas-Elena JV, Obreo J, Wang A, Perez-Barriocanal F, Arevalo M, Bernabeu C, Letarte M, Lopez-Novoa JM.** Reduced angiogenic responses in adult Endoglin heterozygous mice. *Cardiovasc Res* 69: 845–854, 2006.
20. **Jin N, Rhoades RA.** Activation of tyrosine kinases in H_2O_2-induced contraction in pulmonary artery. *Am J Physiol Heart Circ Physiol* 272: H2686–H2692, 1997.
21. **Jones RD, Morice AH.** Hydrogen peroxide–an intracellular signal in the pulmonary circulation: involvement in hypoxic pulmonary vasoconstriction. *Pharmacol Ther* 88: 153–161, 2000.
22. **Kaarteenaho-Wiik R, Kinnula VL.** Distribution of antioxidant enzymes in developing human lung, respiratory distress syndrome, and bronchopulmonary dysplasia. *J Histochem Cytochem* 52: 1231–1240, 2004.
23. **Kawai N, Bloch DB, Filippov G, Rabkina D, Suen HC, Losty PD, Janssens SP, Zapol WM, de la Monte S, Bloch KD.** Constitutive endothelial nitric oxide synthase gene expression is regulated during lung development. *Am J Physiol Lung Cell Mol Physiol* 268: L589–L595, 1995.
24. **Khoo JP, Zhao L, Alp NJ, Bendall JK, Nicoli T, Rockett K, Wilkins MR, Channon KM.** Pivotal role for endothelial tetrahydrobiopterin in pulmonary hypertension. *Circulation* 111: 2126–2133, 2005.
25. **Letteboer TG, Zewald RA, Kamping EJ, de Haas G, Mager JJ, Snijder RJ, Lindhout D, Hennekam FA, Westermann CJ, Ploos van Amstel JK.** Hereditary hemorrhagic telangiectasia: ENG and ALK-1 mutations in Dutch patients. *Hum Genet* 116: 8–16, 2005.
26. **Leung HS, Leung FP, Yao X, Ko WH, Chen ZY, Vanhoutte PM, Huang Y.** Endothelial mediators of the acetylcholine-induced relaxation of the rat femoral artery. *Vascul Pharmacol* 44: 299–308, 2006.
27. **Lin MI, Fulton D, Babbitt R, Fleming I, Busse R, Pritchard KA Jr, Sessa WC.** Phosphorylation of threonine 497 in endothelial nitric-oxide synthase coordinates the coupling of L-arginine metabolism to efficient nitric oxide production. *J Biol Chem* 278: 44719–44726, 2003.
28. **Mata-Greenwood E, Jenkins C, Farrow KN, Konduri GG, Russell JA, Lakshminrusimha S, Black SM, Steinhorn RH.** eNOS function is developmentally regulated: uncoupling of eNOS occurs postnatally. *Am J Physiol Lung Cell Mol Physiol* 290: L232–L241, 2006.
29. **Matoba T, Shimokawa H.** Hydrogen peroxide is an endothelium-derived hyperpolarizing factor in animals and humans. *J Pharm Sci* 92: 1–6, 2003.
30. **Matoba T, Shimokawa H, Nakashima M, Hirakawa Y, Mukai Y, Hirano K, Kanaide H, Takeshita A.** Hydrogen peroxide is an endothelium-derived hyperpolarizing factor in mice. *J Clin Invest* 106: 1521–1530, 2000.
31. **Michelakis ED, Hampl V, Nsair A, Wu X, Harry G, Haromy A, Gurtu R, Archer SL.** Diversity in mitochondrial function explains differences in vascular oxygen sensing. *Circ Res* 90: 1307–1315, 2002.
32. **Nakagiri A, Sunamoto M, Murakami M.** NADPH oxidase is involved in ischaemia/reperfusion-induced damage in rat gastric mucosa via ROS production–role of NADPH oxidase in rat stomachs. *Inflammopharmacology* 15: 278–281, 2007.
33. **North AJ, Star RA, Brannon TS, Ujiie K, Wells LB, Lowenstein CJ, Snyder SH, Shaul PW.** Nitric oxide synthase type I and type III gene expression are developmentally regulated in rat lung. *Am J Physiol Lung Cell Mol Physiol* 266: L635–L641, 1994.
34. **Parker TA, Le Cras TD, Kinsella JP, Abman SH.** Developmental changes in endothelial nitric oxide synthase expression and activity in ovine fetal lung. *Am J Physiol Lung Cell Mol Physiol* 278: L202–L208, 2000.
35. **Pece-Barbara N, Vera S, Kathirkamathamby K, Liebner S, Di Guglielmo GM, Dejana E, Wrana JL, Letarte M.** Endoglin null endothelial cells proliferate faster and are more responsive to transforming growth factor beta1 with higher affinity receptors and an activated Alk1 pathway. *J Biol Chem* 280: 27800–27808, 2005.
36. **Pritchard KA Jr, Ackerman AW, Gross ER, Stepp DW, Shi Y, Fontana JT, Baker JE, Sessa WC.** Heat shock protein 90 mediates the balance of nitric oxide and superoxide anion from endothelial nitric-oxide synthase. *J Biol Chem* 276: 17621–17624, 2001.
37. **Sabba C, Gallitelli M, Pasculli G, Suppressa P, Resta F, Tafaro GE.** HHT: a rare disease with a broad spectrum of clinical aspects. *Curr Pharm Des* 12: 1217–1220, 2006.
38. **Shaul PW, Afshar S, Gibson LL, Sherman TS, Kerecman JD, Grubb PH, Yoder BA, McCurnin DC.** Developmental changes in nitric oxide synthase isoform expression and nitric oxide production in fetal baboon lung. *Am J Physiol Lung Cell Mol Physiol* 283: L1192–L1199, 2002.
39. **Sherman TS, Chen Z, Yuhanna IS, Lau KS, Margraf LR, Shaul PW.** Nitric oxide synthase isoform expression in the developing lung epithelium. *Am J Physiol Lung Cell Mol Physiol* 276: L383–L390, 1999.
40. **Shintaku H, Isshiki G, Hase Y, Tsuruhara T, Oura T.** Normal pterin values in urine and serum in neonates and its age-related change throughout life. *J Inherit Metab Dis* 5: 241–242, 1982.
41. **Srinivasan S, Hanes MA, Dickens T, Porteous ME, Oh SP, Hale LP, Marchuk DA.** A mouse model for hereditary hemorrhagic telangiectasia (HHT) type 2. *Hum Mol Genet* 12: 473–482, 2003.
42. **Suvorava T, Lauer N, Kumpf S, Jacob R, Meyer W, Kojda G.** Endogenous vascular hydrogen peroxide regulates arteriolar tension in vivo. *Circulation* 112: 2487–2495, 2005.
43. **Takahashi S, Mendelsohn ME.** Calmodulin-dependent and -independent activation of endothelial nitric-oxide synthase by heat shock protein 90. *J Biol Chem* 278: 9339–9344, 2003.
44. **Toporsian M, Gros R, Kabir MG, Vera S, Govindaraju K, Eidelman DH, Husain M, Letarte M.** A role for endoglin in coupling eNOS activity and regulating vascular tone revealed in hereditary hemorrhagic telangiectasia. *Circ Res* 96: 684–692, 2005.
45. **Trembath RC, Thomson JR, Machado RD, Morgan NV, Atkinson C, Winship I, Simonneau G, Galie N, Loyd JE, Humbert M, Nichols WC, Morrell NW, Berg J, Manes A, McGaughran J, Pauciulo M, Wheeler L.** Clinical and molecular genetic features of pulmonary hypertension in patients with hereditary hemorrhagic telangiectasia. *N Engl J Med* 345: 325–334, 2001.
46. **Vasquez-Vivar J, Kalyanaraman B, Martasek P, Hogg N, Masters BS, Karoui H, Tordo P, Pritchard KA Jr.** Superoxide generation by endothelial nitric oxide synthase: the influence of cofactors. *Proc Natl Acad Sci USA* 95: 9220–9225, 1998.
47. **Xia Y, Dawson VL, Dawson TM, Snyder SH, Zweier JL.** Nitric oxide synthase generates superoxide and nitric oxide in arginine-depleted cells leading to peroxynitrite-mediated cellular injury. *Proc Natl Acad Sci USA* 93: 6770–6774, 1996.
48. **Yamaguchi K, Asano K, Mori M, Takasugi T, Fujita H, Suzuki Y, Kawashiro T.** Constriction and dilatation of pulmonary arterial ring by hydrogen peroxide–importance of prostanoids. *Adv Exp Med Biol* 361: 457–463, 1994.
49. **Yang Z, Zhang A, Altura BT, Altura BM.** Hydrogen peroxide-induced endothelium-dependent relaxation of rat aorta involvement of Ca^{2+} and other cellular metabolites. *Gen Pharmacol* 33: 325–336, 1999.